since 1961

Baltica

BALTICA Volume 38 Number 1 June 2025: 95–112
https://doi.org/10.5200/baltica.2025.1.8

What types of chemical weathering are effective on rock surfaces for short durations?

Adil Binal

Binal, A. 2025. What types of chemical weathering are effective on rock surfaces for short durations? *Baltica 38 (1)*, 95–112. Vilnius. ISSN 1648-858X.

Manuscript submitted 27 January 2025 / Accepted 6 May 2025 / Available online 19 June 2025

Abstract. Predicting the lifetime of rock materials based on their physical and mechanical properties is essential in engineering geology. This study investigated chemical weathering that may occur after three years in natural building blocks tested in examination tanks at meteorological stations in seven major cities. All tested samples were obtained from quarries within the borders of the Türkiye provinces where the examination tanks were located. X-Ray Fluorescence (XRF), Scanning Electron Microscopy (SEM), thin section examinations, methylene blue tests, capillary water rise tests, and colour change determination analyses were performed at the end of the third year. In a short period, colour changes were observed, and the dissolution of the carbonate rock samples was determined. The capillary level and the weight gain due to capillary water absorption of the field samples was higher than that of the fresh samples. The increase in the electrical conductivity (EC) values of the water accumulated in the examination tank after three years showed that the travertine samples in the tank had dissolved. In addition, the chemical weathering index (CIW)and Parker index (PI) values of the ignimbrite samples exhibit slight changes.

Keywords: *ignimbrite; travertine; colour change; chemical weathering indices; capillary water rise; dissolution*

✉ *Adil Binal (adil@hacettepe.edu.tr)* *https://orcid.org/0000-0002-4183-9430*
Hacettepe University, Faculty of Engineering, Department of Geological Engineering, Beytepe Campus, 06800, Ankara/Türkiye

INTRODUCTION

The alteration of rock surfaces exposed to atmospheric conditions is one of the most fundamental geomorphic processes and is generally called ‘weathering’. Weathering occurs through physical, chemical, and biological processes which result in changes that most commonly weaken the rock surface resulting in what is variously termed rock deterioration, decay, crumbling, decomposition, rotting, disintegration, disaggregation, or breakdown, which leads to erosion of the surface (Hall *et al.* 2012). Rock weathering processes operate synergistically with erosion processes, removing weathered materials to reveal fresh rock surfaces further and continue interacting with atmospheric conditions (Moses *et al.* 2014). Biological activities that depend on bacterial culture accumulation may cause the surface deterioration of silicate and carbonate (Adeli Ghareh Viran, Binal 2018; Dong *et al.* 2022). Generally, descriptive and qualitative methods are used to identify weathering classes of rock materials. An alternative approach to in situ and laboratory testing is to apply standard petrographic techniques and chemical indices to evaluate the successive stages of mineralogical, textural, and chemical changes caused by weathering processes (Cole, Sandy 1980; Tuğrul 2004; Dagdelenler *et al.* 2011). Chemical weathering indices are widely used in modern and old in-situ weathering profile studies. They are sometimes called indices of alteration and are commonly used to characterise weathering profiles. Chemical weathering indices incorporate the bulk major element oxide chemistry into a single value for each sample. They are typically applied by plotting a specific index against depth in a weathering profile, visually representing changes in the bulk chemistry with presumed increasing (or decreasing) weathering of the parent rock (Price, Velbel 2003).

Furthermore, several researchers have investigated the effects of solar radiation on rock. In the heating-cooling type of physical weathering, sunlight radiation causes the daytime heating of stones. The warming and cooling processes are the dominant types of physical weathering in desert environments. As a result of this weathering, rocks expand during the day and shrink at night; microcracks and macrocracks occur on rock surfaces in later stages (Pope *et al.* 2002). Ollier and Clayton (1984) found that an internal pressure of 10 MPa occurred in a rock sample whose temperature increased by 30°C owing to rapid heating. The mineral content is also effective in the heating of rocks. Dark-coloured minerals absorb sunlight faster than light-coloured minerals, and many small stresses occur because of the rapid expansion around dark-coloured minerals. In the last century, extreme increases in air pollution have occurred due to industrialisation and the growth of residential areas. Because of acid rain and aerosols suspended in the air, chemical degradations observed in rock materials in nature for very long periods can occur in residential areas for very short periods. In this study, the effects of atmospheric agents on chemical weathering of traditional rock samples were observed in the field and simulated in a laboratory medium.

MATERIALS AND METHODS

The chemical degradation that may occur after three years in the natural building blocks in the investigation tanks was placed at the meteorological stations of six major cities (Figs 1–2). The physical deterioration of rock samples in the examination tanks was examined in a different study and was published in another article (Binal 2009). All the tested samples were obtained from quarries within the borders of the provinces where the examination tanks were located. Bayburt sandstone was used to represent Erzurum region, which does not belong to that region but is used in the same area as construction material. The samples of Golbasi andesite were analysed to represent the natural building stones utilised in the Ankara region. Aliağa basalt was used to represent Izmir, Bodrum micritic limestone for Muğla, travertine for Afyon, and ignimbrite for Nevsehir. The rock types were identified from the thin sections and X-Ray Diffraction (X-RD) analysis results. The mineral contents of the thin sections are listed in Table 1.

Powder fractions of ten rock samples were prepared for X-RD analysis, and diffractograms were obtained between 2°/min and $2\theta = 5–35°$ for samples with grain sizes smaller than 1 µm. The mineral paragenesis of the aggregates was determined from the characteristic peaks in the diffractograms, and the approximate semi-quantitative mineral percentages of the samples are listed in Table 2. The method Gündoğdu (1982) suggested was used to calculate the semi-quantitative mineral percentages from X-Ray diffractograms.

The water absorption weight and apparent porosity values were determined to observe the effect of the physical properties on the chemical weathering. Physicomechanical tests were performed according to the methods recommended by the ISRM (2015). The highest water absorption by weight and apparent porosity values were observed for black ignimbrite samples. The lowest values were detected in the basalt and micritic limestone samples (Table 3).

UV rays effect test

The colours of rocks used in current structures and historical monuments are essential parameters in architecture and engineering. In addition, colour has always been an evaluation tool for rock descriptions and rock weathering classifications by engineering

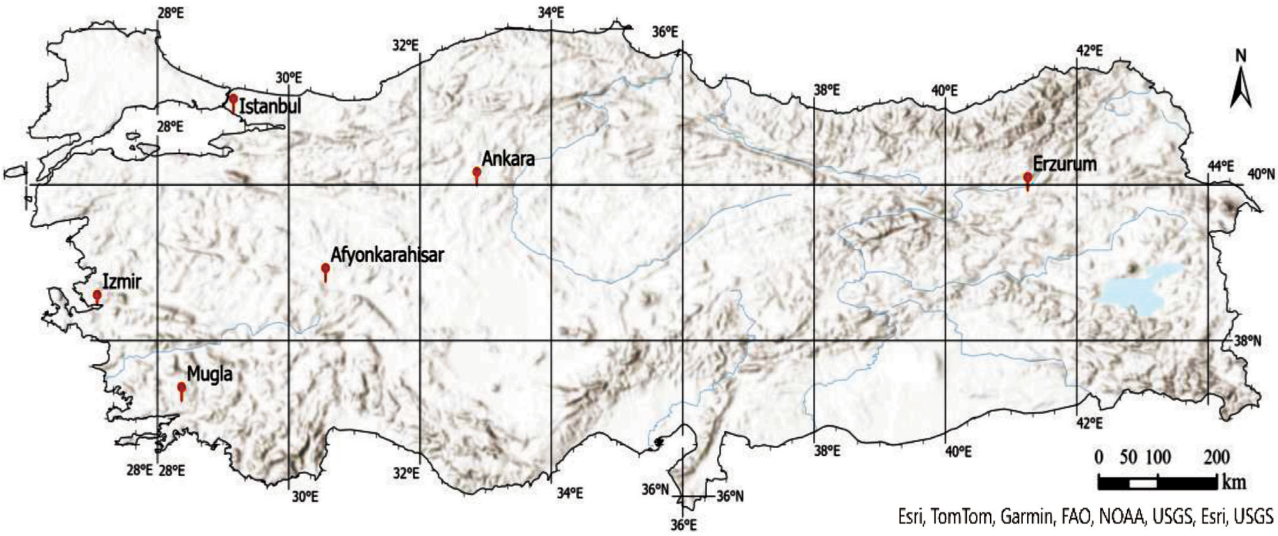

Fig. 1 Locations of the investigation tanks (red dots) in the territory of Türkiye

geologists. The colour of the rock is mainly affected by the tint of its minerals, matrix, and grain size. The external surface colours of stones used as exterior cladding materials change due to atmospheric effects. The factors that cause colour changes are aerosols from the atmosphere, such as carbon dioxide (CO_2), ozone (O_3), sulphates (SO_2, SO_3), nitrate (NO_x), and UV rays from the sun (Winkler 1966). The electromagnetic energy emitted from the sun can be divided into three types: ultraviolet (UV) rays, visible, and

City	Sample	The views of investigation tanks at the meteorological stations	City	Sample	The views of investigation tanks at the meteorological stations
Nevsehir	Ignimbrites		Izmir	Basalt	
Ankara	Andesite		Erzurum	Sandstone	
Muğla	Micritic Limestone		Afyon	Travertine	

Fig. 2 Research tanks and natural building stones

Table 1 Thin section examinations

Rock Type	Texture	Matrix / Ash / Lithic Fragments	Phenocrysts
Ignimbrite (black)	Eutaxitic	It contains fibrous pumice, and the grain sizes of the fiamme are small. Ash is glassy rock fragments of volcanic origin	Plagioclase, clinopyroxene
Ignimbrite (red)	Eutaxitic	It contains fibrous pumice, and the grain sizes of the fiamme are small. Ash is glassy rock fragments of volcanic origin	Plagioclase, clinopyroxene
Ignimbrite (brown)	Eutaxitic	Fiamme structures and recrystallised pumices, ash is glassy mainly in nature, with traces of devitrification after deposition. Rock fragments of volcanic origin	Plagioclase, clinopyroxene
Ignimbrite (greenish grey)	Vitrophyric	Lithic fragments	Plagioclase, opaque minerals
Ignimbrite (grey)	Vitrophyric	There are very few plagioclase microliths. In general, volcanic glass predominates. There are traces of post-depositional devitrification (Y- and S-shaped glass splinters)	Plagioclase
Andesite	Hypo-crystalline porphyritic	Trachytic texture Matrix: volcanic glass, plagioclase microliths, amphibole and opaque mineral microcrystals	Plagioclase, amphibole
Micritic limestone			Thin calcite veins are present (secondary calcites). Quartz minerals are present. The grains are very fine
Basalt	Hypo crystalline porphyritic	Intersertal texture, volcanic glass + plagioclase microliths + clinopyroxene + olivine microcrystals	Plagioclase: volcanic glass + microlith + microcrystal inclusions, in cumulates olivine, clinopyroxene
Sandstone			Plagioclase, quartz, biotite, clinopyroxene, opaque minerals
Travertine			There are calcite, quartz, and biotite minerals. Silica is present in the voids

Table 2 Summary of the semi-quantitative analysis of the whole-rock mineralogy of rock types based on X-RD

Rock Type	Quartz	Feldspar	Calcite	Opal-Ct	Mica	Kaolinite	Clay
Ignimbrite (black)	12	56	2	15	–	–	25
Ignimbrite (red)	11	18	–	51	–	–	19
Ignimbrite (brown)	1	50	–	29	–	–	20
Ignimbrite (greenish grey)	2	18	–	63	–	–	18
Ignimbrite (grey)	–	31	–	50	7	–	12
Micritic limestone	11	24	45	–	–	–	35
Basalt	2	48	–	25	–	–	25
Sandstone	26	5	18	–	13	30	7
Andesite	3	60	–	–	–	–	38
Travertine	1	–	99	–	–	–	–

Table 3 Apparent porosity and water absorption by weight of tested samples

Rock Type	*Water Absorption by Weight (%)	Standard Deviation	*Apparent Porosity (%)	Standard Deviation	No
Ignimbrite (black)	15.67	0.65	28.52	1.15	16
Ignimbrite (red)	10.11	0.19	20.52	0.44	16
Ignimbrite (brown)	12.10	0.34	23.58	0.58	16
Ignimbrite (greenish grey)	12.99	0.45	25.76	1.00	16
Ignimbrite (grey)	6.80	0.34	14.36	0.69	16
Micritic limestone	0.26	0.06	0.71	0.16	32
Basalt	0.23	0.10	0.61	0.27	23
Sandstone	9.39	0.47	19.52	0.85	44
Andesite	3.76	0.12	8.35	0.27	51
Travertine	2.81	0.81	6.80	1.82	30

* Average values, No: Number of samples.

infrared. Infrared energy has a longer wavelength than visible red light and starts at approximately 760 nm. The visible-light region was between 400 and 760 nm. Ultraviolet light has a wavelength of less than 400 nm (Michel, Rots 2022). The International Commission on Light (CIE) divides the UV spectrum of sunlight into three subsections according to wavelength (Fig. 3).

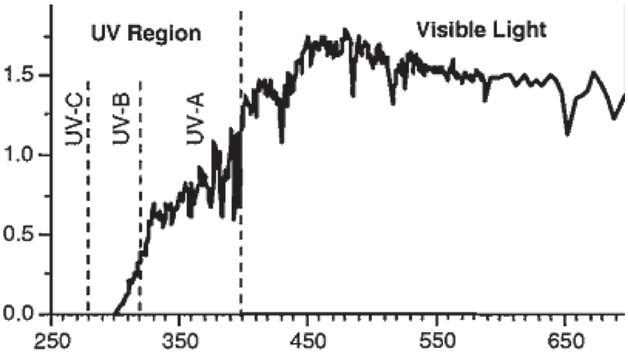

Fig. 3 Sunlight spectrum (Brennan, Fedor 1988)

Table 4 Relative radiation energies of UV beams on Earth (Cockell 1998)

UV Rays	Watt/m^2
UV-C (100–280 nm)	~ 0
UV-B (280–315 nm)	3.7
UV-A (315–400 nm)	71.3

UV-C, which has the lowest wavelength among these rays, has a destructive effect on the cell structures of living organisms. Almost all this radiation is absorbed by ozone in the upper layers of the atmosphere. A small part of UV-B rays, which have other harmful effects on living organisms, pass through the ozone layer and reach the Earth. UV-A rays have the highest radiation energy among UV rays reaching the Earth because most of them pass through the ozone layer (Cockell 1998). However, UV-C rays are absorbed by the atmosphere and reflect nearly zero radiation energy to the Earth (Table 4).

Several studies have evaluated the effects of solar radiation on rocks, typically in terms of physical weathering (Blackwelder 1933; Brennan, Fedor 1988; Jenkins, Smith 1990; Gómez-Heras *et al.* 2006; Silva *et al.* 2022). Few studies have been conducted on colour changes caused by sunlight in rocks. Winkler (1966) stated that colour lightening occurs in grey limestones and shales under sunlight and that black limestones and marbles turn from black to dull-dirty-grey. The 10-year monthly solar energy values for Ankara are presented in Table 5. It reached its highest solar energy level in July and lowest energy level in December.

A new experimental setup was developed to examine the colour changes of rock samples under ultraviolet light in a laboratory environment. The experimen-

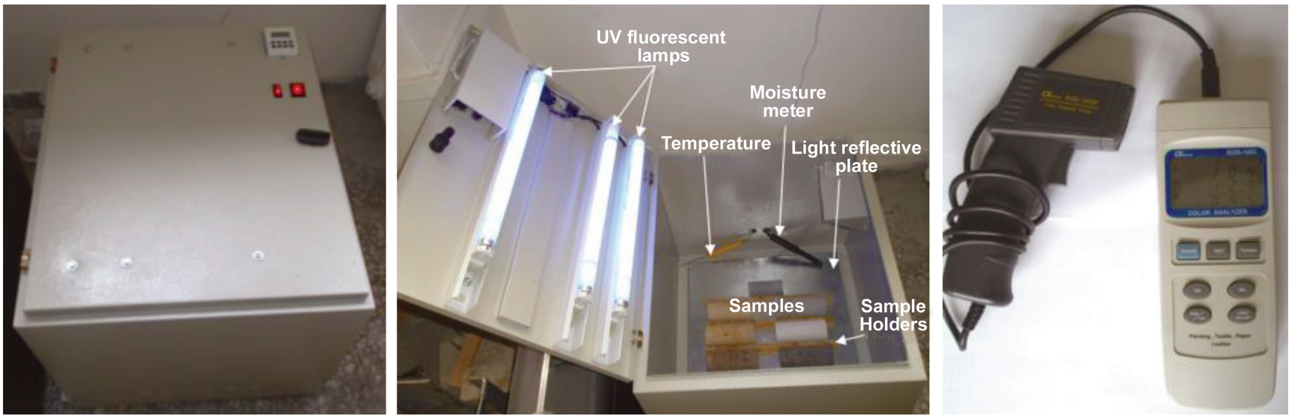

(a) (b) (c)

Fig. 4 UVA and UVB rays' experimental setup (a), internal view of the device (b), and colour analyser that measures the colours of objects without light sources (c)

Table 5 The average monthly solar energy of Ankara (location: 39'57" N, 32'53" E) (Whitlock *et al.* 2000)

Months	Ave. Sun Radiation (kWh/m^2/day)
January	1.77
February	2.38
March	3.69
April	4.54
May	5.53
June	6.63
July	6.99
August	6.55
September	5.22
October	3.24
November	1.99
December	1.51
Annual Average	4.17

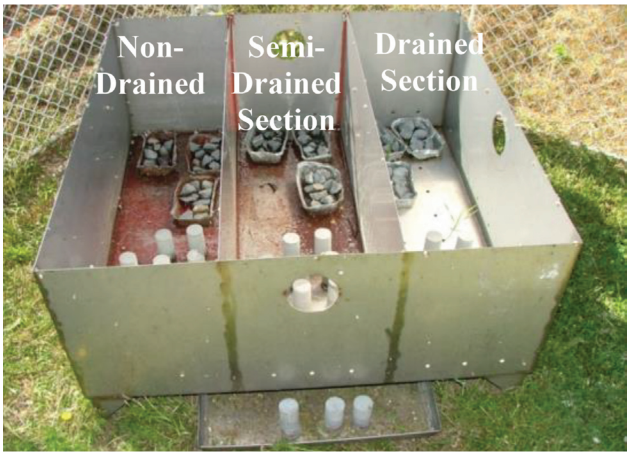

Fig. 5 Investigation tank and specimens placed at the Muğla meteorological station

tal setup was placed in a steel cell and consisted of a UV light source and ambient humidity, temperature, and UV light radiation meters (Fig. 4a). Three fluorescence lights of 20 Watt each applied an average of 100 µW of UV light energy to the cm² of the samples at 50 cm (Fig. 4b). The ventilation holes at the bottom of the cell were closed during the experiment to maintain constant environmental conditions such as temperature and humidity inside the cabinet. The colour changes occurring in the samples during monthly periods were detected using a portable colour analyser with three primary colour sensors with a 10-bit resolution, which analyses the colour of objects that are not light sources (Fig. 4c). This measures colours by dividing them into red, green, and blue bands (RGB), and can also determine the saturation, brightness, and hue values of the measured colours. In the experimental setup, one side was continuously exposed to UV rays, and the back surface was left in the dark. Colour measurements of the samples were performed constantly from a fixed area on the rock sample. In addition, the UV light radiation, humidity, and temperature inside the experimental setup were determined during the measurements. Colour measurements were made in the laboratory for six months. The average temperature in the experimental setup was 19.5°C, the average relative humidity was 34.5%, and the average UV radiation produced by the fluorescents was 300 µW/cm². Field measurements showed that solar UV radiation varies between 200 and 500 µW/cm² at noon in cloudy, windless weather and between 800 and 1600 µW/cm² on sunny days.

The colour changes observed in the samples stored in the field were compared with laboratory results. Colour measurements were made over a six-month period on the samples kept in the field examination tanks located at the Nevsehir, Muğla, Izmir, Erzurum, Ankara, and Afyon meteorological stations (Fig. 5). An examination tank consists of compartments with three different water drainage systems. Rainwater accumulated in the first section because water drainage was not allowed, and the samples generally remained damp. In the middle compartment, rainwater can rise to a certain level and is then discharged through holes on the sides of the compartment. In the last compartment, the samples generally remained dry because of water drainage holes at the bottom and sides.

The RGB values measured from the surfaces of the rock samples were first converted into X, Y and Z values, using the equations given below (Eq. 1, 2 and 3) in accordance with the ASTM D 2244 colour tolerance and colour difference determination standard.

$$X = 0.4124\left(\frac{R + 0.055}{1.055}\right)^{2.4} + 0.3576\left(\frac{G + 0.055}{1.055}\right)^{2.4} + + 0.1805\left(\frac{B + 0.055}{1.055}\right)^{2.4} \tag{1}$$

$$Y = 0.2126\left(\frac{R + 0.055}{1.055}\right)^{2.4} + 0.7152\left(\frac{G + 0.055}{1.055}\right)^{2.4} + + 0.0722\left(\frac{B + 0.055}{1.055}\right)^{2.4} \tag{2}$$

$$Z = 0.0193\left(\frac{R + 0.055}{1.055}\right)^{2.4} + 0.1192\left(\frac{G + 0.055}{1.055}\right)^{2.4} + + 0.9505\left(\frac{B + 0.055}{1.055}\right)^{2.4} \tag{3}$$

Here: R: red, G: green, B: blue.

The X, Y, and Z values were converted into L, a, and b values, which are another colour definition, based on fluorescence light values (X_n: 103.28, Y_n: 100, and Z_n: 69.026) and using equations (4, 5, and 6) given in the ASTM D 2244 standard.

$$L = 116\left(\frac{Y}{Y_n}\right)^{1/3} - 16 \tag{4}$$

$$a = 500\left[\left(\frac{X}{X_n}\right)^{1/3} - \left(\frac{Y}{Y_n}\right)^{1/3}\right] \tag{5}$$

$$b = 200\left[\left(\frac{Y}{Y_n}\right)^{1/3} - \left(\frac{Z}{Z_n}\right)^{1/3}\right] \tag{6}$$

The difference between the L, a, and b colour values of the samples before and after the experiment was determined from the equation given below (Eq. 7), according to ASTM D 2244.

$$E_{ab} = \sqrt{(\Delta L)^2 + (\Delta a)^2 + (\Delta b)^2} \tag{7}$$

The red, green, and blue (RGB) colour spectra of the samples kept in the field examination tank and the UV test setup in the laboratory were measured using a colour analyser. The colour analyser reads primary colours between 0 and 1024. The R: 1024, G: 1024, and B: 1024 values corresponded to white, whereas R = 0, G = 0, and B = 0 corresponded to black. The colour lightness (H), saturation (S), and illumination (L) values varied between 0 and 1.

Methylene blue test

The methylene blue test was used to determine whether clay minerals developed because of chemical degradation on the surfaces of the samples kept in the examination tanks. Methylene blue is an organic dye with acidic characteristics that is used in many disciplines, such as analytical chemistry, biology, and medicine. As in the areas mentioned above, it is used as a practical index test method in engineering design, although it is not directly intended for design because of its adsorption features. Methylene blue was used as a redox indicator in analytical chemistry. Although it has a colour close to red when dry, it turns dark blue-blue when dissolved in water. Because of this colour, it is also called dark blue methylene. Methylene blue (MB), a heterocyclic compound, is a ring-structured organic compound with the chemical formula $C_{16}H_{18}CIN_3S$. The type and specific surface area of clay minerals contained in rocks can be estimated using the methylene blue (MB) test. In methylene blue clay mineral interactions, methylene blue anions replace the cations in the clay mineral. This reaction continues until they balance each other. As a result of this reaction, the cation exchange capacity (CEC) was determined (Yool *et al.* 1998). The surface areas of the clays were also determined using the methylene blue test. The clay minerals have different surface areas. Methylene blue covers clay minerals as a single-molecule (monomolecular) layer. As a result of this interaction, the surface area of clay minerals can be determined (Çokça 1991).

The methylene blue experiment was performed using two different methods: spot and spectrophotometric methods. In this study, the clay content of the samples was estimated from the colour differences left by methylene blue on the samples and the distribution of halos formed in the spot experiments. Dihydrate methylene blue (4.28 g) in powder form was mixed with 1000 ml of pure or deionised water. Dried powdered rock samples (2 g) were suspended in 25 ml of pure water. Then, 25 ml of water were added to the mixture and mixed using a mixer. First, 1 ml of the methylene blue solution was mixed with the prepared mixture. The mixture was dropped onto a filter paper using a pipette or stick. Methylene blue (0.5 ml of methylene blue) was then added to the solution. It was then dropped onto the filter paper. At the beginning of the experiment, drops were observed in dark blue colour. The dripping process was continued until a lighter halo was formed around the dark circle. After a halo was observed, the solution at the same concentration was mixed in a mixer for 1 min and then drops were added again. The test was considered complete when a halo was observed (Fig. 6).

The volume of methylene blue consumed: MBV = V_{cc}/F for 100g, V_{cc}: amount of methylene blue injected into the solution (cc), F: weight of the sample used (g).

Capillary water rise experiment

The capillary water level rise experiments of the samples were also carried out, and the capillary water rises of fresh specimens and those kept in the field for three years were compared. Throughout the tests, the reasons for the rise in the capillary water level and the increase in the capillary water level owing to degradation were examined. The core samples with a diameter of 54 mm and length of 120 mm were prepared for the capillary water-rise test. Before the experiment, the samples were dried in an oven at 105°C for 24 h and then placed on 2 cm thick plastic supports such that their bottom parts did not touch the bottom of the tray in which they were placed. Water was added to the tray to a depth of 2.5 cm. The samples (0.5 cm) from the bottom were in contact with the water (Fig. 7).

The rising capillary water levels along the outer surfaces of the samples and their weights were measured at periods of 1, 2, 4, 8, 10, 15, 30, and 60 min and 2, 4, 8, 12, and 24 h. During the field observations, the capillary water level in the samples kept in the compartment where water drainage was not allowed was measured for six months. Simultaneously, capillary water rise experiments were conducted on samples from the field in the laboratory environment.

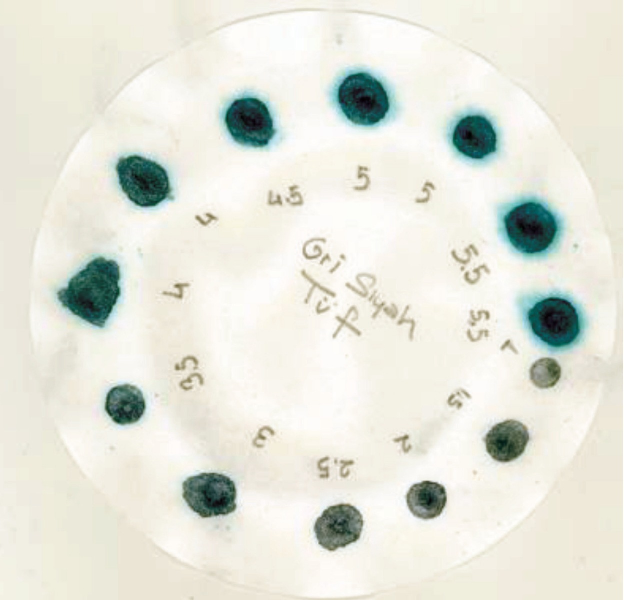

Fig. 6 Methylene blue experiment application (ign. black)

Fig. 7 Capillary water rise experiment of andesite samples

Chemical analysis

Chemical analyses were performed on fresh rock samples exposed to atmospheric conditions for three years. Chemical weathering index values were determined based on the major oxide values. The Ruxton ratio (RO), Parker index (PI), modified weathering potential index (MWPI) and chemical weathering index (CIW) were calculated based on the data obtained in this study. Based on these values, information on the stability of fresh rock samples and the degree of weathering of rock samples decomposed under atmospheric conditions for three years. The equations for the chemical indices are presented (Table 6).

Table 6 Chemical weathering indices

Indices	Formulae	References
RO	SiO_2/Al_2O_3	Ruxton 1968
PI	$2Na_2O/0.35 + MgO/0.90 + 2K_2O/0.25 + CaO^*/0.70$	Parker 1970
MWPI	$[Na_2O + K_2O + CaO + MgO] \times 100/$ $[Na_2O + K_2O + CaO + MgO + SiO_2 + Al_2O_3 + Fe_2O_3]$	Vogel 1975
CIW	$[Al_2O_3 \times 100]/[Al_2O_3 + CaO^* + Na_2O]$	Harnois 1988

RO: Ruxton ratio, PI: Parker index, MWPI: modified weathering potential index, CIW: chemical weathering index, CaO*: content of CaO incorporated in silicate fraction.

In the equations mentioned above, the primary oxides are represented in molar proportions, and CaO* refers to the amount of CaO present in the silicate portion. McLennan (1993) introduced an indirect approach to estimating the CaO content in the silicate fraction by assuming plausible Ca/Na ratios for silicate materials. The method for determining the CaO content (CaO*) in the silicate fraction involved deducting the molar proportion of P_2O_5 from the total molar proportion of CaO. If, after this deduction, the "remaining number of moles" is less than the molar proportion of Na_2O, then this "remaining number of moles" is considered the molar proportion of CaO in the silicate fraction. Conversely, if the "remaining number of moles" exceeds the molar proportion of Na_2O, then the molar proportion of Na_2O is regarded as the molar proportion of CaO in the silicate fraction (CaO*) (McLennan 1993; Cho, Ohta 2022).

In the weathering classification of the indices, the upper and lower values of fresh and weathered rocks and their relationship with the degree of weathering were investigated by Price and Velbel (2003) (Table 7).

Table 7 Chemical degradation indices (Price, Velbel 2003)

Index	Optimum Fresh Value	Optimum Degraded Value	Trend of the Index Value as the Degree of Degradation Increases
RO	> 10	0	Negative
PI	> 100	0	Negative
CIW	≤ 50	100	Positive

SEM analyses

Rock samples were taken after three years after the section where water drainage was not allowed. Small pieces weighing approximately 5 g were obtained from the samples in contact with water and from the surface. The pieces were viewed under an electron microscope and an attempt was made to obtain information about the degradation.

Rainwater accumulated in examination tanks

The atmosphere had a very little corrosive effect on stone without water. However, the washing of aggressive components from the atmosphere with rainwater increases corrosion and stone solution. Dissolved CO_2, SO_2, SO_3, and Cl were the most effective abrasives. The urban atmosphere provides much more CO_2 and sulphates through the combustion of fossil fuels than the atmosphere in rural areas, which greatly accelerates stone decay in urban areas. Water with few ions in solution can be as corrosive as water loaded with CO_2 and SO_4, as it actively reaches an equilibrium state with the stone in contact. Silicate rocks can resist long-term exposure to rainwater (Winkler 1966). Samples were collected from rainwater accumulated in the compartments of the study tanks, where water drainage was not allowed (Fig. 8). The major oxides in the water samples were examined over three years.

Fig. 8 View of travertine samples kept in the undrained section of the investigation tank at the Afyon Meteorological Station

RESULTS

Colour changes

Colour change graphs were prepared based on the laboratory and field assessments. The values 1, 2, 3, 4, 5, and 6 on the horizontal axis represent the monthly colour measurements conducted in the laboratory. The terms undrained, semi-drained, and drained correspond to the colour measurements obtained from samples in the respective compartments after three years. The samples were exposed to UV-A and UV-B rays in the laboratory; after 180 days, whitening occurred in the dark-coloured rock samples (basalt and micritic limestone), and there was not much change in the surface colour of the light-coloured travertine samples (Fig 9a). The colour of the sandstone sample darkened slightly owing to the decrease in the RGB and illumination values (Fig 9b).

In dark-coloured rock samples, particularly basalt samples, lightening in colour was detected owing to the increase in RGB and illumination values (Fig. 10a–h). Among the samples in the different compartments of the field examination tank, the highest colour lightening was observed on the surfaces of the samples in the drained (D.) compartment. Samples in the compartment where drainage was not allowed (non-D.) or in the compartment with partial permission (Semi-D.) generally remain moist, solar radiation is less effective, and less discoloration occurs on surfaces.

The appearance of the samples in which the effect of UV rays was determined in the laboratory at the end of the six-month experimental period is shown in Figs 11–12. The colour of the samples was continuously measured from a fixed area on the rock sample. One surface of each sample was constantly exposed to UV rays, whereas the other remained in the dark. In particular, the colour fading observed in basalt samples can be detected visually.

As a result of the laboratory experiments, the colour lightening seen especially in basalt (colour change rate: 8.24) and dark grey micritic limestone (colour change rate: 17.06) samples became detectable even with the eye. Fewer colour changes were observed in the black and red ignimbrite samples, which have high visible porosity and water absorption values by weight. A darkening in colour was observed in the travertine and sandstone samples tested as light-coloured rock samples and the ratios were determined as 13.8 and 20.99 according to Equation 7. More colour changes were observed in the samples kept in the field examination tank under atmospheric conditions for three years compared to the samples tested in the laboratory (Table 8).

In particular, the colour changes observed in the samples kept in the compartment where water drainage was allowed were greater than those observed

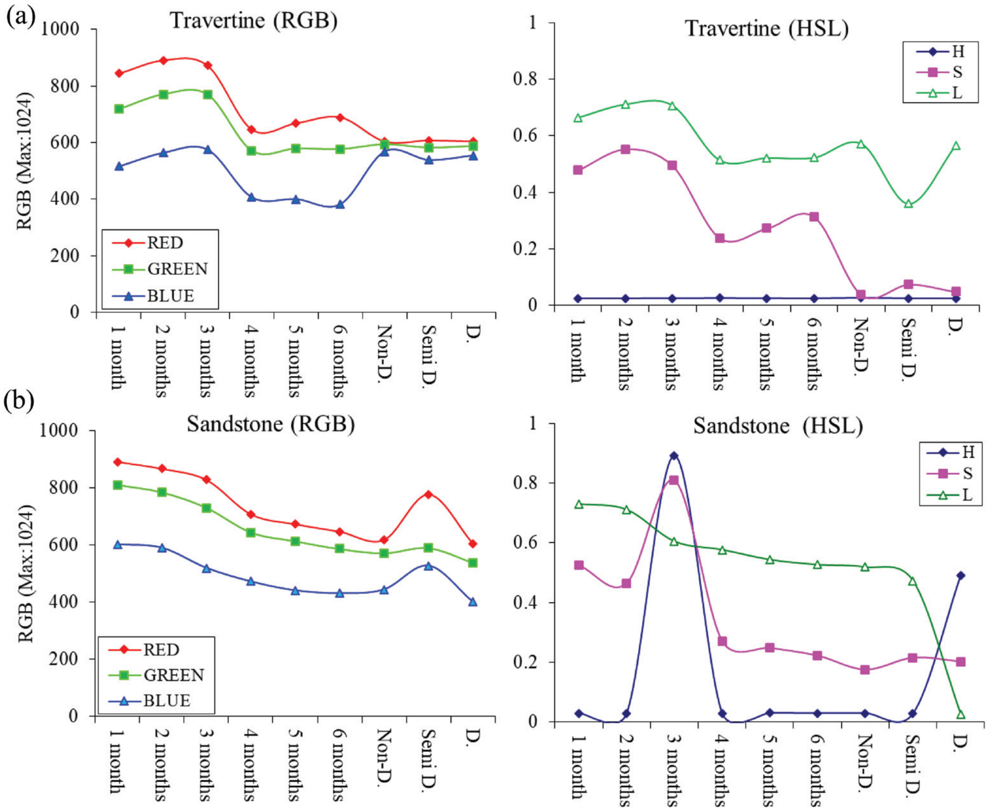

Fig. 9 RGB and HSL values of light-coloured rock samples: a) travertine and b) sandstone

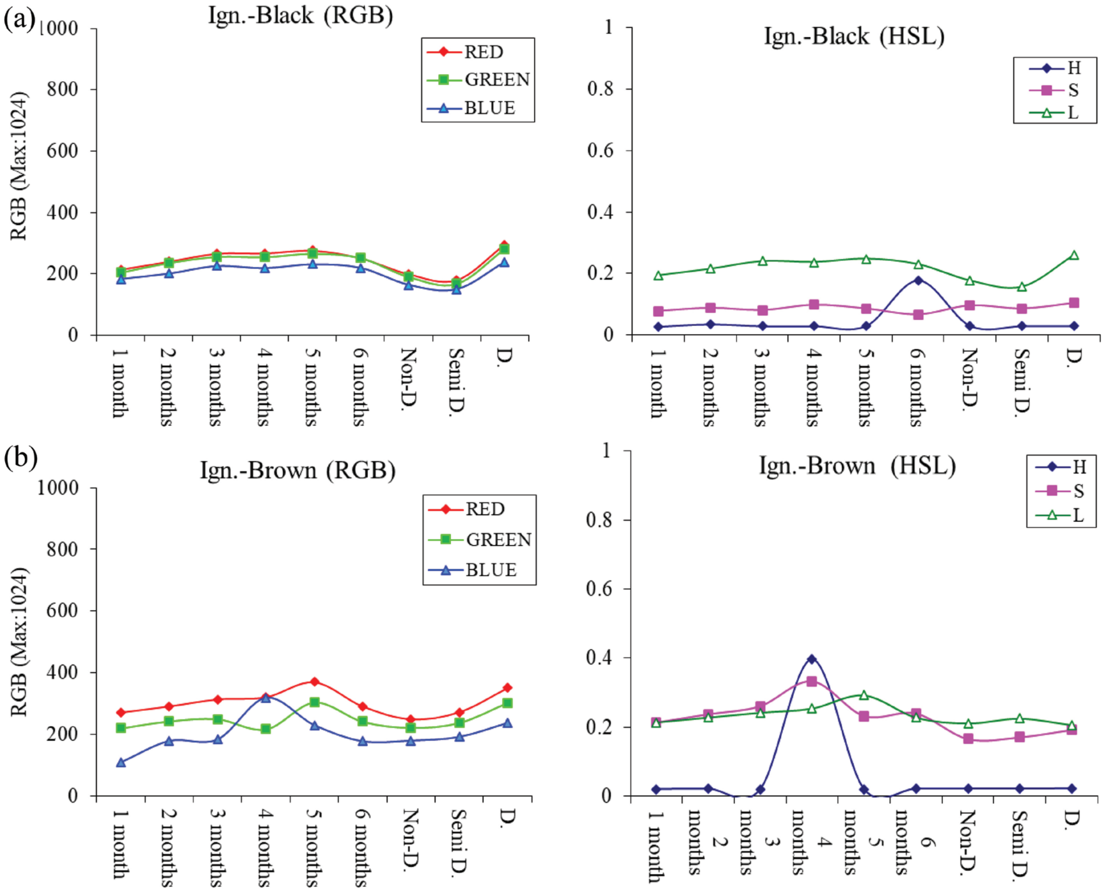

Fig. 10 RGB and HSL values of the dark rock samples, a) ignimbrite (black), b) ignimbrite (brown), c) ignimbrite (red), d) ignimbrite (grey), e) ignimbrite (greenish grey), f) basalt, g) andesite, h) micritic limestone (continue)

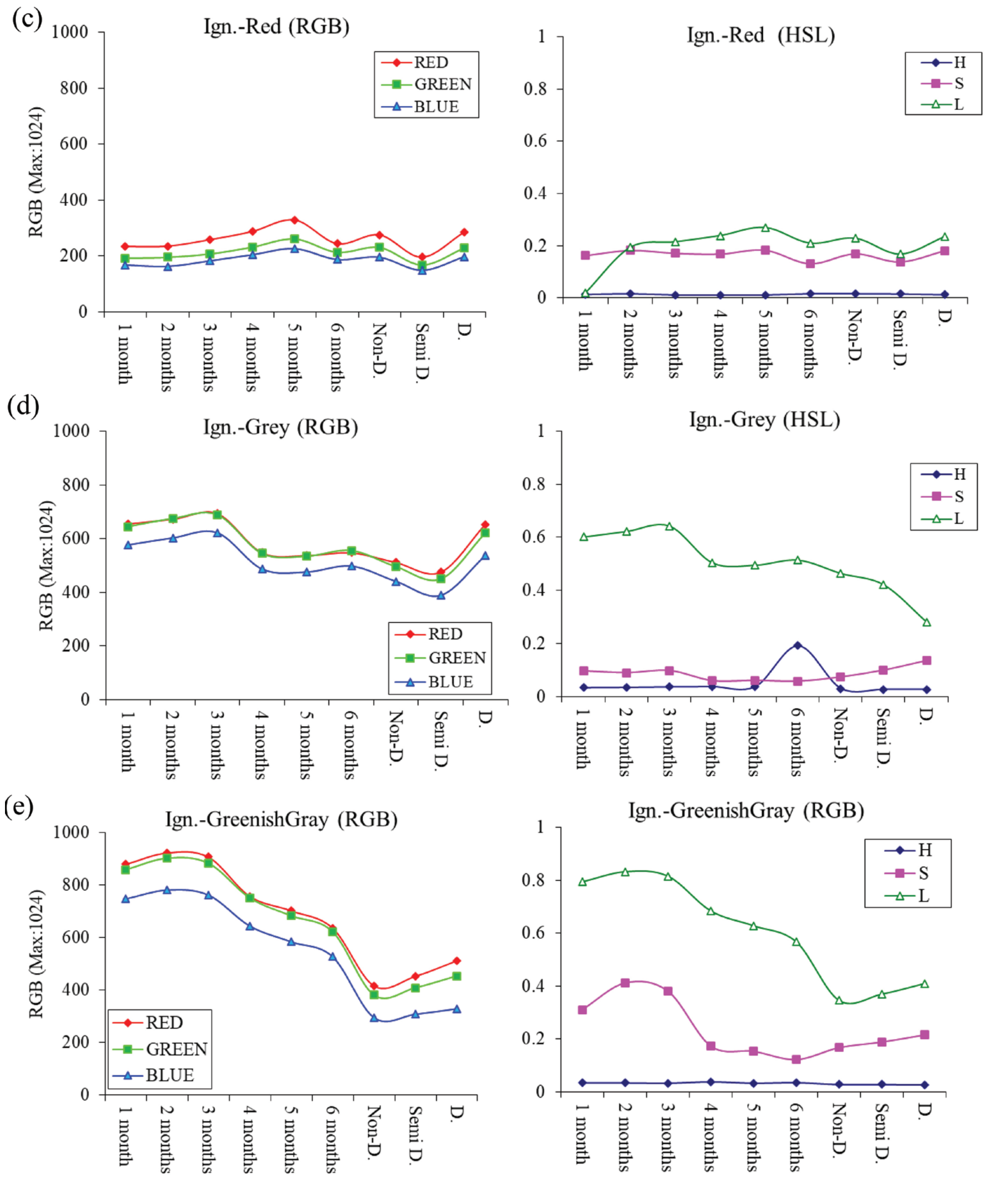

Fig. 10 RGB and HSL values of the dark rock samples: a) ignimbrite (black), b) ignimbrite (brown), c) ignimbrite (red), d) ignimbrite (grey), e) ignimbrite (greenish grey), f) basalt, g) andesite, h) micritic limestone (continue)

Table 8 The variation in the rock colour (Eq. 7, ASTM D 2244) at the end of three years in the field and after six months of laboratory testing

Colour	Sample	Lab. (6 months)	Non-D	Semi-D	D
	Ignimbrite (red)	2.83	4.39	3.34	4.52
	Ignimbrite (black)	5.41	2.19	4.38	8.61
Dark	Basalt	8.24	3.19	5.17	4.96
	Ignimbrite (brown)	9.63	13.39	13.10	14.60
	Micritic limestone	17.06	5.38	10.70	21.60
	Andesite	6.11	17.64	18.52	22.44
Light	Travertine	13.80	30.12	27.30	28.90
	Sandstone	20.99	23.19	26.77	25.61

in the other compartments. The reason for the lower colour changes in the laboratory environment is that the UV fluorescence of the experimental setup cannot generate as much UV radiation energy as that of the sun. The highest colour lightening in the field was observed for basalt (4.96), brown ignimbrite (14.6), and micritic limestone (21.6). Darkening occurred mostly in travertine (28.9) and sandstone (25.61) samples. The colour change in the travertine samples in the field (28.9) is much greater than the amount of colour

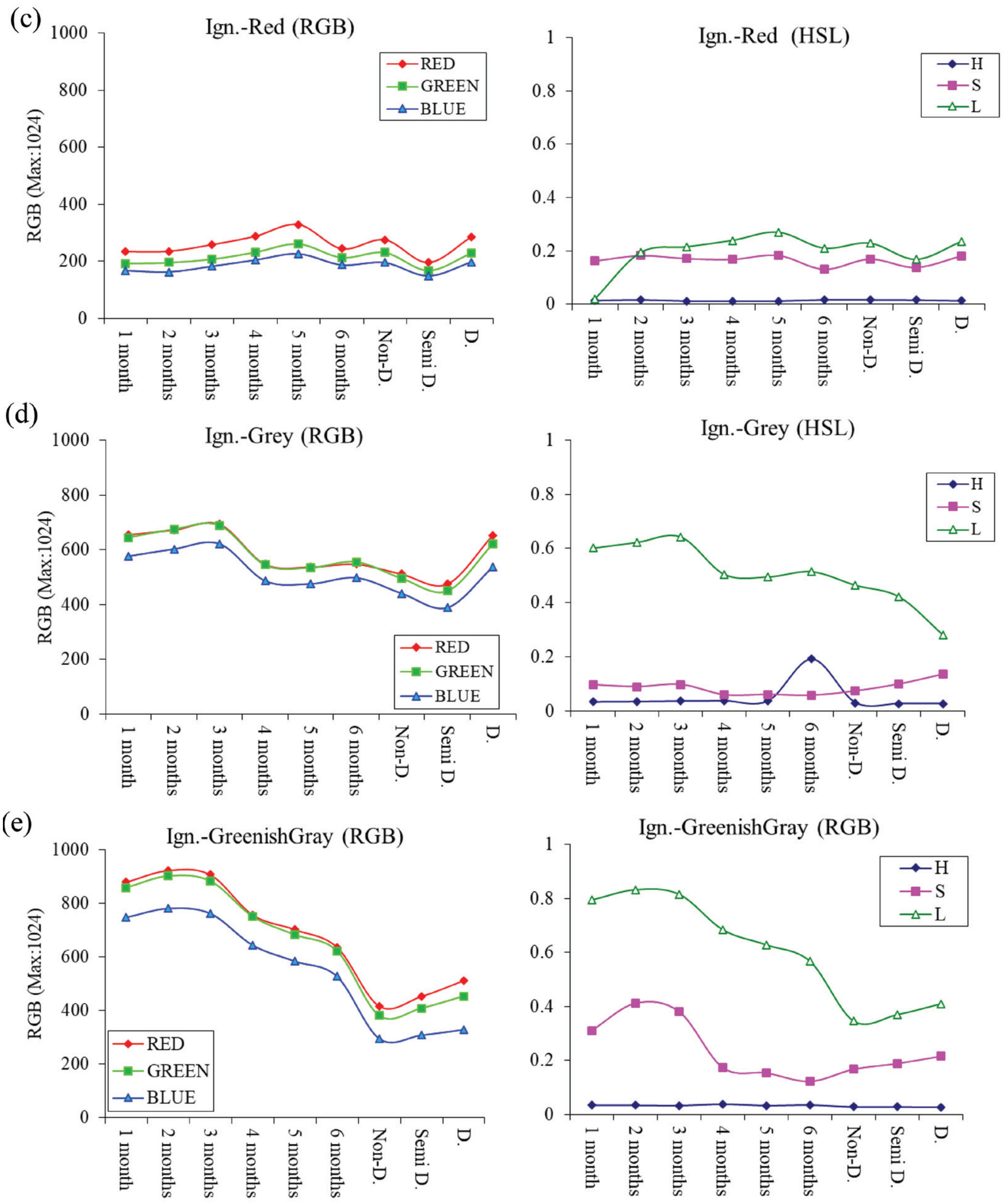

Fig. 10 RGB and HSL values of the dark rock samples: a) ignimbrite (black), b) ignimbrite (brown), c) ignimbrite (red), d) ignimbrite (grey), e) ignimbrite (greenish grey), f) basalt, g) andesite, h) micritic limestone (continue)

changes in the travertine samples tested in the laboratory (13.8), which can be attributed to the effect of UV rays and the dissolution of the travertine samples by rainwater in the natural environment.

Methylene blue spot

Methylene blue spot tests were conducted on samples exposed to atmospheric conditions for three years. The minimum methylene blue absorption and cation exchange capacity were determined in the basalt samples. The highest values were obtained for the sandstone and andesite samples (Table 9). The results confirmed the clay content selected by the XRD analysis. The highest clay content in the XRD

Table 9 Methylene blue test results of samples kept in the field for three years

Sample	Vcc	MBV
Ign. (black)	5	2.5
Ign. (red)	2.5	1.25
Ign. (brown)	2.5	1.25
Ign. (greenish grey)	3.5	1.75
Ign. (grey)	4.5	2.25
Micritic limestone	2	1
Basalt	1.5	0.75
Sandstone	8	**4**
Andesite	6.5	**3.25**
Travertine	3.5	1.75

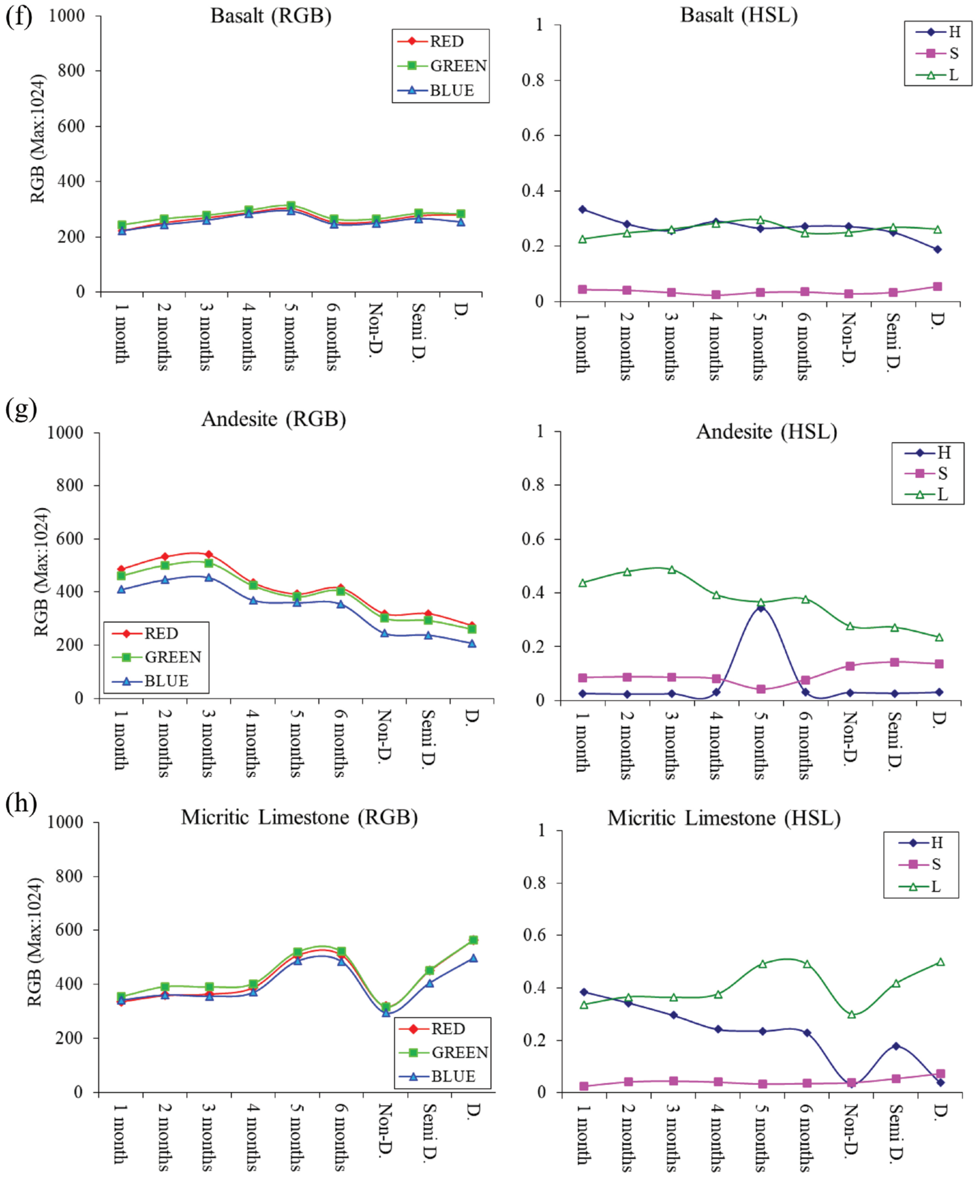

Fig. 10 RGB and HSL values of the dark rock samples: a) ignimbrite (black), b) ignimbrite (brown), c) ignimbrite (red), d) ignimbrite (grey), e) ignimbrite (greenish grey), f) basalt, g) andesite, h) micritic limestone (continue)

analyses was detected in sandstone (kaolinite: 30% + 7% clay) and andesite (38%) samples. In carbonate rocks, there is an interaction between methylene blue and calcium carbonate, leaving a pinkish colour on the filter paper. This was thought to be due to the acidic properties of methylene. It was also observed that when mixed with methylene, the lime dissolved and rose to the surface. Therefore, it was concluded that the methylene blue spot test does not provide reliable results for clayey rocks containing calcium carbonate or rock samples with basic characteristics.

Capillary water rise

The capillary water rise values of the fresh samples were compared with those of the decomposed samples obtained in the field. The increase in capillary water level along the outer surfaces of fresh samples, those exposed to atmospheric effects in the field for three years, and the weight increase of the samples due to water absorption during the experiment were determined. These samples were not tested because capillary water rise did not occur in travertine and micritic limestone samples. The highest increase in the capillary water level occurred in the ignimbrite samples, and the lowest in the basalt samples (Fig. 13a). The weight gain values of the samples were parallel to the increase in capillary water level values. The ignimbrite samples exhibited the highest weight gain owing to water absorption (Fig. 13b). At the same time, there was a more significant difference between the weight gain values of the fresh ignimbrite samples and field ignimbrite samples compared to the other samples. In general, more substantial weight gain and increased capillary water levels were detected in samples kept in the field.

Chemical Indices

The Ruxton ratio and Parker index were high in fresh rock and low in residual soil. The significant decrease in the Parker index is related to the determination of this index based on the ratios of alkaline earth metals with high mobility. However, there is no regular change in the modified weathering potential index from fresh rock to the ground (Tuğrul 1995). The dissolution of rock samples (travertine and micritic limestone) containing minerals dissolved by carbonic acid, such as calcite, was examined within the scope of the project, and samples were collected from rainwater accumulated in the examination tanks because of rain. The changes in major elements in the water samples were examined, and we attempted to obtain information about whether there was any dissolution in the rock samples. The chemical analysis of the rock samples was performed, and the major oxide values were determined (Tables 10–11). The ratios were completed to 100%, and the chemical weathering index values were calculated.

The chemical indices of the samples kept under atmospheric conditions for three years were calculated and compared with those of the fresh rock samples (Fig. 14a). The degree of chemical degradation of the samples was determined based on the ignition loss values. However, slight changes were observed in the ignition losses of the samples (Fig. 14b).

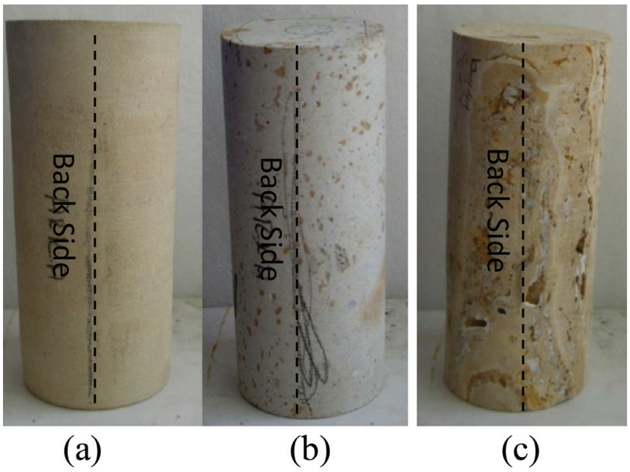

Fig. 11 View of light-coloured rock samples tested under UV light in the laboratory after six months: a) sandstone, b) ign. (greenish grey), and c) travertine

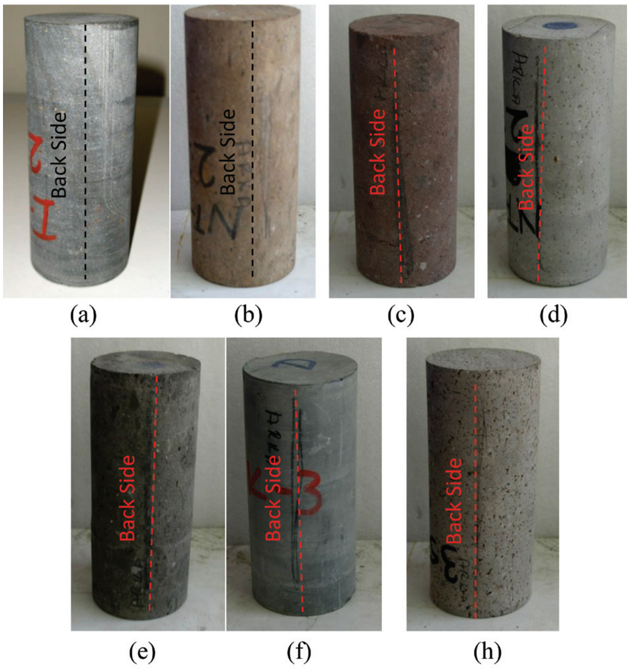

Fig. 12 Appearance of dark rock samples tested under UV light in the laboratory after six months: a) basalt, b) ign. (brown), c) ign. (red), d) ign. (grey), e) ign. (black), f) micritic limestone, and h) andesite

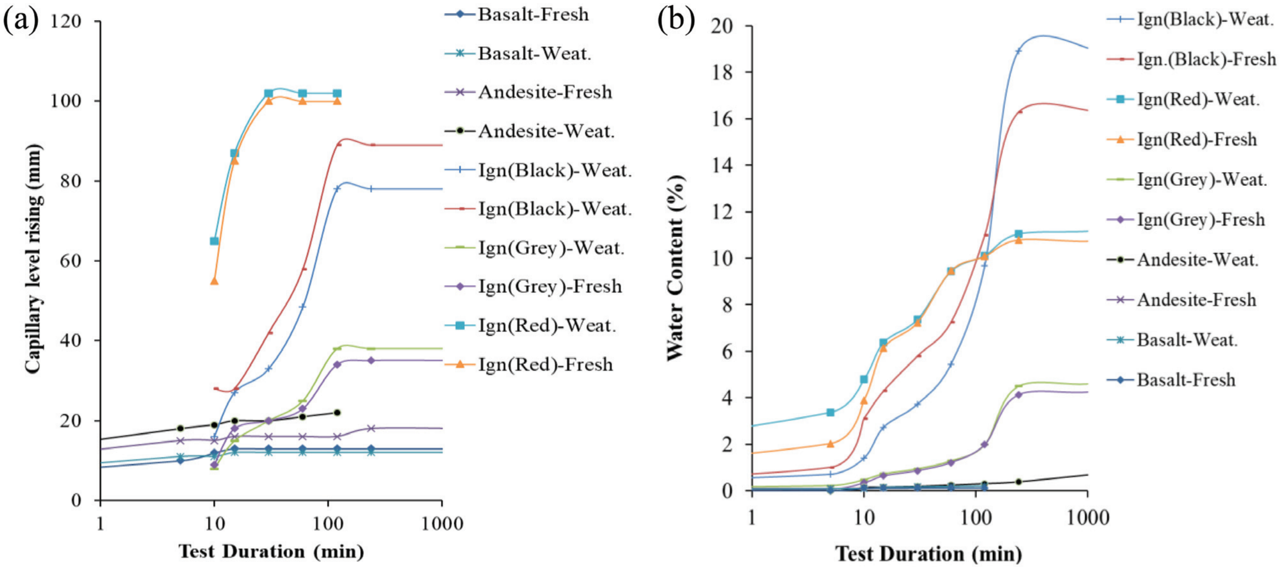

Fig. 13 Capillary water level rise of the samples (a), water contents with capillary water level rise (b)

Table 10 Chemical analysis of the main elements resulted in the oxide values of the tested rock samples

Sample	Na_2O	MgO	Al_2O_3	SiO_2	P_2O_5	K_2O	CaO	CaO*	TiO_2	MnO	Fe_2O_3	LOI
Ign. (black)	4.5	1.0	15.9	64.9	0.2	2.7	3.2	3.0	0.7	0.1	4.4	2.4
Ign. (red)	4.2	18.4	13.5	51.7	0.3	1.4	4.1	3.9	0.8	0.1	5.0	0.5
Ign. (brown)	4.9	1.1	16.0	64.1	0.2	2.5	3.3	3.1	0.8	0.1	4.6	2.4
Ign. (greenish grey)	5.2	0.2	14.7	71.8	0.1	3.3	1.9	1.8	0.4	0.1	1.3	0.9
Ign. (grey)	5.1	0.3	14.4	72.5	0.1	3.5	1.3	1.2	0.3	0.1	1.8	0.6
Micritic limestone	0.2	0.6	1.3	10.3	0.1	0.2	49.5	0.2	0.1	0.1	0.9	36.8
Basalt	3.4	3.8	14.9	59.2	0.2	2.0	7.4	3.4	0.5	0.1	6.5	1.9
Sandstone	0.4	0.5	11.7	61.2	0.1	0.8	10.2	0.4	0.3	0.1	3.0	11.7
Andesite	5.1	0.5	17.4	63.8	0.5	2.3	4.1	3.6	0.7	0.1	4.8	0.7
Travertine	0.1	0.5	1.9	6.7	0.1	0.4	50.7	0.1	0.1	0.1	0.8	38.6

LOI: loss on ignition (1000°C), CaO*: content of CaO incorporated in silicate fraction.

Table 11 Major oxide values (%) of samples kept in the field for three years

Sample	Na_2O	MgO	Al_2O_3	SiO_2	P_2O_5	K_2O	CaO	CaO*	TiO_2	MnO	Fe_2O_3	LOI
Ign. (black)	4.3	1.0	15.7	64.8	0.2	2.5	3.5	3.3	0.7	0.1	4.7	2.5
Ign. (red)	4.1	18.5	13.4	51.7	0.3	1.3	4.2	3.9	0.8	0.1	5.1	0.6
Ign. (brown)	4.8	1.2	15.9	64.1	0.2	2.4	3.5	3.3	0.7	0.1	4.7	2.4
Ign. (greenish grey)	5.1	0.2	14.7	71.9	0.1	3.2	2.0	1.9	0.4	0.1	1.4	1.0
Ign. (grey)	5.0	0.3	14.7	72.9	0.1	3.0	1.1	4.2	0.3	0.1	1.9	0.6
Micritic limestone	0.2	0.6	1.3	10.3	0.1	0.2	49.6	0.2	0.1	0.1	0.9	36.6
Basalt	3.3	4.0	14.7	58.8	0.2	2.0	7.8	3.3	0.5	0.1	6.8	1.9
Sandstone	0.3	0.5	11.6	61.1	0.1	0.7	10.4	0.3	0.3	0.1	3.1	11.9
Andesite	5.0	0.5	17.2	63.5	0.5	2.2	4.7	1.0	0.7	0.1	4.9	0.7
Travertine	0.1	0.6	2.0	6.8	0.1	0.4	49.5	0.1	0.1	0.1	0.9	39.3

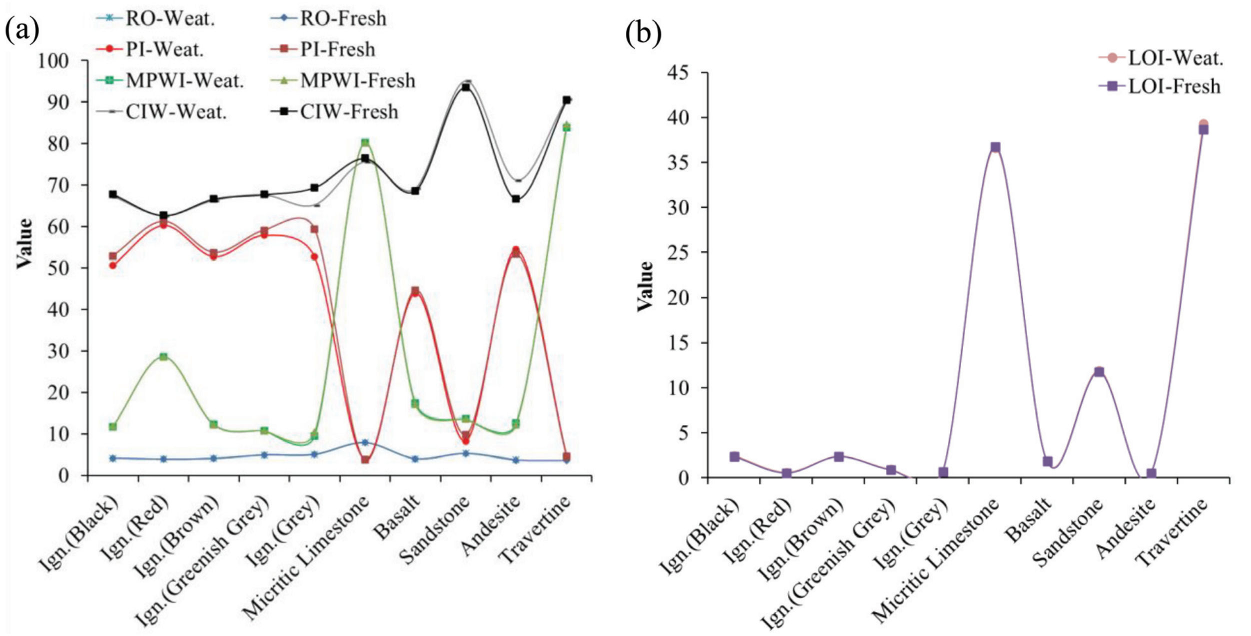

Fig. 14 Chemical degradation index values of the tested samples (a) and loss of ignition values of fresh and field samples (b) RO: Ruxton ratio, PI: Parker index, MWPI: modified weathering potential index, CIW: chemical weathering index, CaO*: content of CaO incorporated in silicate fraction

SEM analysis

Fractures were observed in the feldspar minerals of the basalt samples owing to physical weathering (Fig. 15a). Kaolinizations were determined for feldspar minerals in the sandstone samples (Fig. 15b). Alterations were detected in the volcanic glass of the ignimbrite (brown) sample (Fig. 15c). No weathering or fractures were observed in the calcite minerals of the micritic limestone samples (Fig. 15d). There was no space between calcite

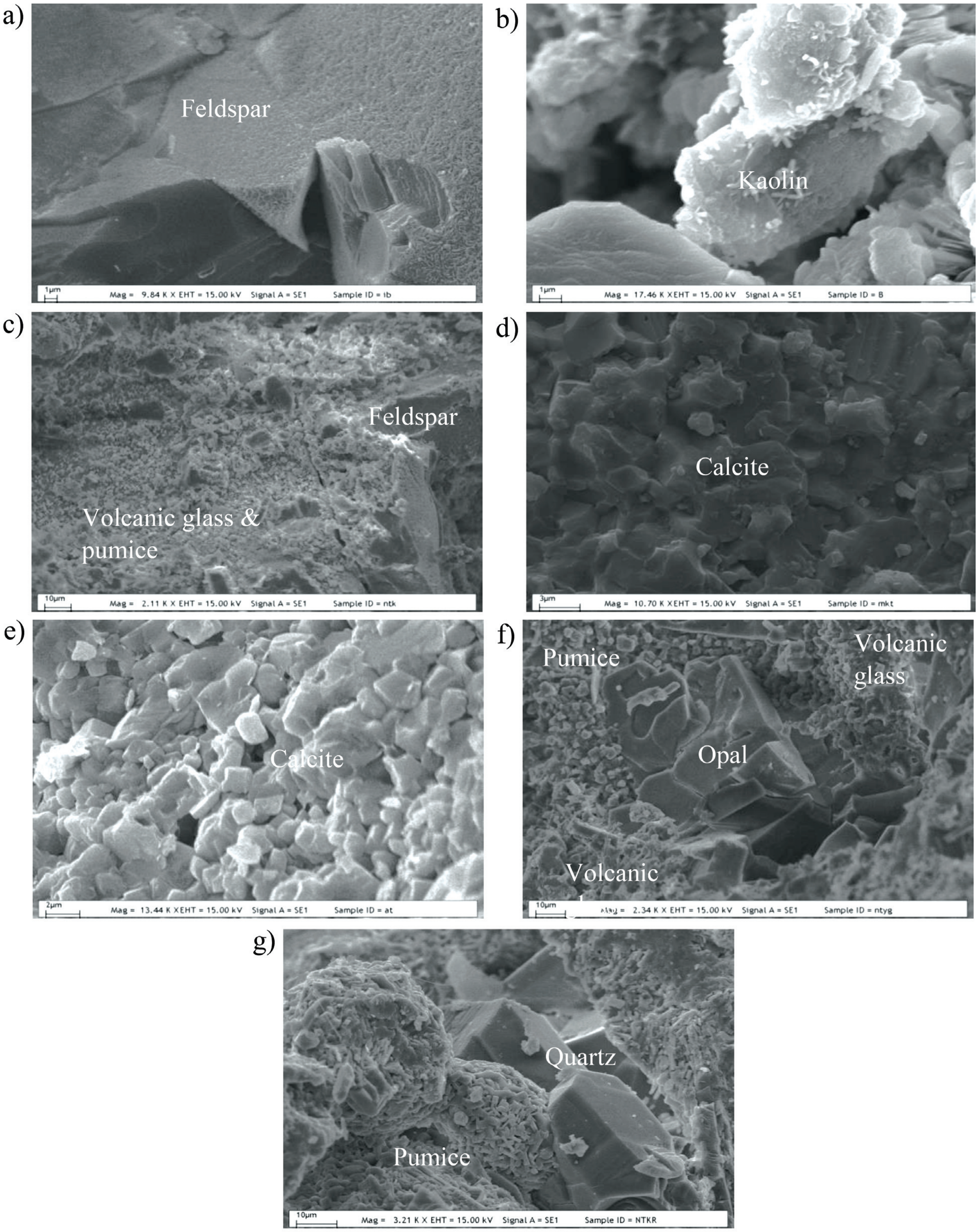

Fig. 15 SEM images of the samples after three years of field tests: a) fractures in feldspar minerals in basalt, b) feldspar and kaolin minerals in sandstone, c) ignimbrite (brown), d) micritic limestone, e) travertine, f) ignimbrite (greenish grey), g) ignimbrite (red)

minerals. In the SEM image of the travertine sample, gaps between calcite minerals were identified. Distortions in the mineral shape and rounding of the mineral corners were detected because of the dissolution around the calcite grains (Fig.15e). Fractures on the surface of the opal minerals and decomposition in the pumice volcanic glass splinters were detected in the SEM image of the ignimbrite (greenish grey) sample (Fig. 15f). No degradation of quartz minerals was observed in the ignimbrite (red) SEM image (Fig. 15g).

Water chemistry analysis

The results of the sandstone, ignimbrite, and travertine samples with high changes in water chemistry are shown in Fig. 16. Travertine samples kept in the undrained compartment in Afyon lost more weight because of dissolution than those in the other compartments. This was confirmed by analysing the water samples collected from the undrained sections. The EC and carbonate content values were higher than those of the water samples from other provinces. High EC (µs/cm) values indicated that the examined travertine was dissolved. The pH measurements varied from 6.2 to 9.42 (Table 12). In the Nevşehir region, there was a decline in the pH from 7.09 to 6.2. In contrast, the Ankara region exhibited an increase in pH within the tank containing andesite samples, rising from 7.95 to 9.42, which signifies an alkaline condition. Significant sulphate (SO_4) levels were identified, notably in Afyon (268 ppm) and Nevsehir (358 ppm), most likely due to the air pollution characteristic of urban areas.

CONCLUSIONS

The surface changes in the samples kept in the field for three years were determined. Colour measurements were made on rock samples kept under atmospheric conditions for three years and tested under UV light in the laboratory. The highest colour lightening in the field was observed for basalt (4.96), brown ignimbrite (14.6), and micritic limestone (21.6). Darkening occurred mostly in travertine (28.9) and sandstone (25.61) samples. The colour change in the travertine samples in the field (28.9) is much greater than the amount of colour changes in the travertine samples tested in the laboratory (13.8), which can be attributed to the effect of UV rays and the dissolution of the travertine samples by rainwater in the natural environment. Among the samples located in the vari-

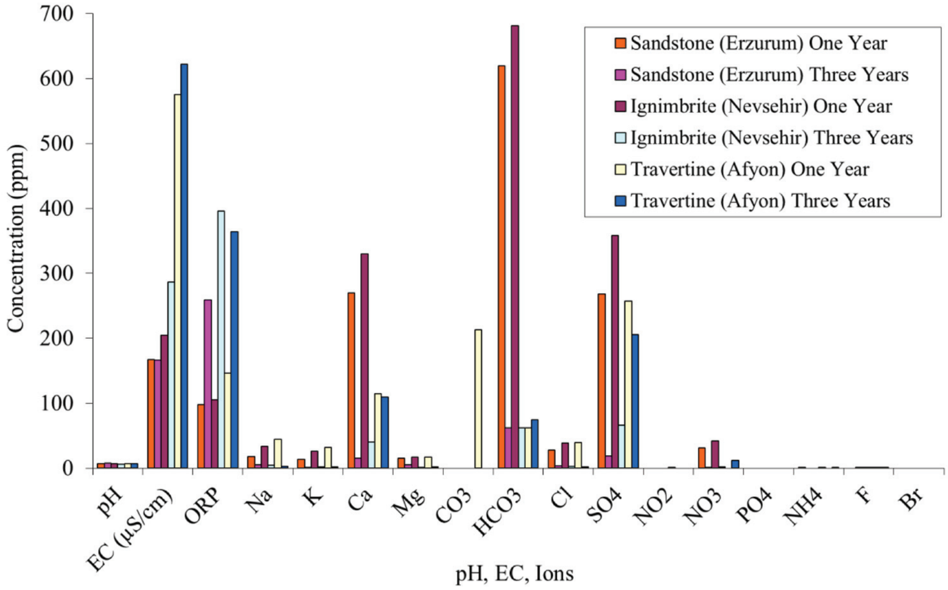

Fig. 16 Chemical analysis of water accumulated in the compartments of the examination tanks, where water drainage was not allowed

Table 12 Water chemistry analysis

Location	pH	EC(µS/cm)	ORP	*Na	K	Ca	Mg	HCO_3	Cl	SO_4	NO_2	NO_3	PO_4	NH4	F	Br	
Nevşehir	7.09	205	105.3	33	26	330	17	681	39	358	< 0.01	42	< 0.01	< 0.01	0.12	< 0.01	First year
Afyon	7.3	575	146	44	32	114	17	62	40	257	< 0.01	< 0.01	< 0.01	< 0.01	0.23	< 0.01	
Erzurum	7.4	167	98.1	18	14	270	15	619	28	268	< 0.01	31	< 0.01	0.22	< 0.01	< 0.01	
Muğla	8.05	137	125.8	1.78	0.67	21.95	1.09	52.64	2.34	16.86	< 0.01	< 0.01	< 0.01	0.125	0.03	< 0.01	
İzmir	8.67	134	1217	5.51	1.60	18.01	1.64	40.44	8.35	21.03	< 0.01	< 0.01	< 0.01	< 0.01	0.05	< 0.01	
Ankara	7.95	229	26.6	7	1	29	1	54	8	34	0.02	0.04	0.16	0.35	0.11	< 0.01	
Nevşehir	6.2	287	396.2	4.37	2.11	40.10	1.57	61.93	2.44	66.53	0.16	2.13	< 0.01	1.19	0.25	< 0.01	After 3 years
Afyon	7.31	622	364.4	2.62	1.99	109.66	1.68	74.31	1.97	205.6	< 0.01	11.65	< 0.01	0.27	0.75	< 0.01	
Erzurum	7.73	166	258.7	5.32	1.45	15.61	5.71	61.93	3.58	19.07	< 0.01	0.64	< 0.01	< 0.01	0.16	< 0.01	
Muğla	7.72	130	290.0	1.92	0.93	20.63	0.44	1.10	4.18	23.32	0.01	1.39	0.00	0.16	0.06	0.009	
İzmir	7.92	133	287.4	4.98	2.13	16.36	1.31	1.10	11.50	13.78	0.00	1.66	0.00	0.15	0.05	0.027	
Ankara	9.42	354	277.4	11.29	2.37	50.87	2.09	86.96	86.96	71.07	< 0.01	< 0.01	0.07	< 0.01	0.08	0.074	

* All values are in ppm. CO_2 was measured only in Afyon. This value was 230 ppm.

ous compartments of the field examination tank, the most significant colour lightening was observed on the surfaces of the samples within the drained (D.) compartment. In contrast, solar radiation is less effective in reducing discolouration on their surface samples from compartments where drainage was not permitted (non-D.) or partially allowed (semi-D) and remained moist. The effects of UV light can also be used as an input parameter for weathering classification, and more comprehensive research should be conducted on this subject.

Samples taken from the surfaces of the samples brought from the field were ground into a powder, and a methylene blue spot test was applied. The values obtained from the experiments were consistent with the X-Ray diffractograms. The highest methylene blue absorption and cation exchange capacity were observed in sandstone (MBV: 4) and andesite samples (MBV: 3.25) with high clay content.

In the capillary water rise experiments, the rise in capillary water and weight gain along the outer surfaces of the samples whose bottom bases were in contact with water were determined. When the test results of the fresh and field samples were compared, it was determined that the increase in capillary water level and weight gain in the ignimbrite samples exposed to atmospheric conditions were higher. Microcrack development increases over time and water reaches the inner parts of the rock material, resulting in an increase in the capillary water level because of physical and chemical weathering. The ignimbrite samples exhibited the highest water content, with an increase of up to 17.1% compared with the fresh samples.

Chemical analyses of the samples collected from the fresh and examination tanks were performed, and the major oxide values were determined. The Ruxton ratio, Parker index, modified weathering potential index, and chemical weathering index, which are chemical indices, were calculated. The Ruxton ratios of the samples stored in the field differed slightly from those of fresh samples. The Ruxton ratio is calculated from the change in SiO_2 content, and there is a possibility of a minimal shift in the silicon oxide content in such a short time. No change was observed in the chemical indices' values of the basalt and micritic limestone samples compared with those of the fresh samples. Although the Parker index values of the ignimbrite samples were very low, they showed a change compared with the fresh samples. Owing to the clay content, slight changes were observed in the modified weathering potential index values of the andesite and sandstone samples. It was determined that there was a slight increase in the loss of ignition values of the ignimbrite samples stored in the field compared with the fresh samples.

Samples were taken for SEM and chemical analysis from the external surfaces in contact with the water of the samples that were exposed to atmospheric effects for three years in the field and kept in a compartment where water drainage was not allowed. In the travertine samples, rounding of the mineral corners and increased spaces between the minerals were observed, owing to the dissolution of calcite minerals. Less deformation or degradation of calcite minerals in the micritic limestones was detected in the SEM images compared with the travertine samples. Minimal degradation was observed in the volcanic glass shards that formed the pumices of the ignimbrite samples.

Rainwater accumulates in compartments where drainage is not permitted. Water samples were collected from this compartment in six-month periods. The major oxides in the water samples, electrical conductivity (EC), and pH were also determined. The EC (622 μS/cm) values in the water samples from the examination tank containing travertine samples were higher than those from the other tanks. A high EC value indicates dissolution of the travertine samples. The sulphate values were high in the water samples collected from the examination tanks in Afyon (257 ppm) and Nevsehir (358 ppm). This shows that sulphate originates from rainfall in large cities due to air pollution.

As a result, dissolution-type chemical weathering in carbonate rocks over short periods, increased capillary water following the development of microcracks in porous volcanic sedimentary stones, and colour lightening in dark-coloured rock samples have been detected.

ACKNOWLEDGEMENT

This study was funded by the Turkish National Scientific Committee, TUBITAK (Project No: 106Y296). I sincerely thank the editor and reviewers for taking the time to review my manuscript and providing constructive feedback to improve my manuscript.

REFERENCES

Adeli Ghareh Viran, P., Binal, A. 2018. Effects of Repeated Freeze-Thaw Cycles on Physico-Mechanical Properties of Cohesive Soils. *Arabian Journal of Geosciences 11(11)*. https://doi.org/10.1007/s12517-018-3592-5

Binal, A. 2009. A New Laboratory Rock Test Based on Freeze-Thaw Using a Steel Chamber. *Quarterly Journal of Engineering Geology and Hydrogeology 42(2)*, 179–198. https://doi.org/ 10.1144/1470-9236/08-040

Blackwelder, E. 1933. The Insolation Hypothesis of Rock Weathering. *American Journal of Science*s *5–26(152)*. https://doi.org/10.2475/ajs.s5-26.152.97

Brennan, P., Fedor, C. 1988. Sunlight, UV and Accelerated Weathering. *Additives for Polymers 18(7)*. https://doi.org/10.1016/0306-3747(88)90432-0

Cho, T., Ohta, T. 2022. A robust chemical weathering index for sediments containing authigenic and biogenic materials. *Palaeogeography, Palaeoclimatology, Palaeoecology 608, 111288*. https://doi.org/10.1016/j.palaeo.2022.111288

Cockell, C.S. 1998. Biological Effects of High Ultraviolet Radiation on Early Earth-a Theoretical Evaluation. *Journal of Theoretical Biology 193(4)*. https://doi.org/10.1006/jtbi.1998.0738.

Çokça, E. 1991. *Swelling Potential of Expansive Soils with a Critical Appraisal of the Identification of Swelling of Ankara Soils by Methylene Blue Tests*. PhD. Thesis, Ankara: Middle East Technical University [In Türkiye].

Cole, W.F., Sandy M.J. 1980. A Proposed Secondary Mineral Rating for Basalt Road Aggregate Durability. *Australian Road Research 10(3)*, 27–37.

Dagdelenler, G., Akcapinar, S.E., Gokceoglu, C. 2011. Some Non-Linear Models to Predict the Weathering Degrees of a Granitic Rock from Physical and Mechanical Parameters. *Expert Systems with Applications 38(6)*, 7476–7485. https://doi.org/10.1016/j.eswa.2010.12.076

Dong, Z., Pan, X., Tang, C., Shi, B. 2022. Microbial Healing of Nature-like Rough Sandstone Fractures for Rock Weathering Mitigation. *Environmental Earth Sciences 81(15)*, 394. https://doi.org/10.1007/s12665-022-10510-w

Gómez-Heras, M., Smith, B.J., Fort, R. 2006. Surface temperature differences between minerals in crystalline rocks: Implications for granular disaggregation of granites through thermal fatigue. *Geomorphology, 78(3–4)*, 236–249. https://doi.org/10.1016/j.geomorph.2005.12.013

Gündoğdu, N. M. 1982. *Neojen yaşlı Bigadiç sedimanter baseninin jeolojik, mineralojik ve jeokimyasal incelenmesi*. Hacettepe University, PhD thesis, Ankara [In Turkish].

Hall, K., Colin, T., Sumner, P. 2012. On the Persistence of Weathering. *Geomorphology 149–150*, 1–10. https://doi.org/10.1016/j.geomorph.2011.12.024

Harnois, L. 1988. The CIW Index: A New Chemical Index of Weathering. *Sedimentary Geology 55(3–4),* 319–322. https://doi.org/10.1016/0037-0738(88)90137-6

ISRM 2015. *The ISRM Suggested Methods for Rock Characterization, Testing and Monitoring: 2007–2014*. Ulusay, R. *et al*. (eds). Springer International Publishing. https://doi.org/10.1007/978-3-319-07713-0

Jenkins, K.A., Smith, B.J. 1990. Daytime Rock Surface Temperature Variability and Its Implications for Mechanical Rock Weathering: Tenerife, Canary Islands. *CATENA 17(4–5)*, 449–459. https://doi.org/10.1016/0341-8162(90)90045-F

Michel, M., Rots, V. 2022. Into the Light: The Effect of UV Light on Flint Tool Surfaces, Residues and Adhesives. *Journal of Archaeological Science: Reports 43*, 103479. https://doi.org/10.1016/j.jasrep.2022.103479

McLennan, M.S. 1993. Weathering and global denudation. *The Journal of Geology 101(2)*, 295–303. http://dx.doi.org/10.1086/648222

Moses, C., Robinson, D., Barlow, J. 2014. Methods for Measuring Rock Surface Weathering and Erosion: A Critical Review. *Earth-Science Reviews 135*, 141–161. https://doi.org/10.1016/ j.earscirev.2014.04.006

Ollier, C., Clayton, K.M. 1984. *Weathering*. 2nd ed. Longman, London.

Parker, A. 1970. An Index of Weathering for Silicate Rocks. *Geological Magazine 107(6)*, 501–504. https://doi.org/10.1017/S0016756800058581

Pope, G.A., Meierding, T.C., Paradise, T.R. 2002. Geomorphology's Role in the Study of Weathering of Cultural Stone. *Geomorphology 47(2–4)*, 211–225. https://doi.org/10.1016/S0169-555X(02)00098-3

Price, J.R., Velbel, M.A. 2003. Chemical Weathering Indices Applied to Weathering Profiles Developed on Heterogeneous Felsic Metamorphic Parent Rocks. *Chemical Geology 202(3–4)*, 397–416. https://doi.org/10.1016/j.chemgeo.2002.11.001

Ruxton, B.P. 1968. Measures of the Degree of Chemical Weathering of Rocks. *The Journal of Geology 76(5)*, 518–527. https://doi.org/10.1086/627357

Silva, T.P., de Oliveira, D., Veiga, J.P., Lisboa, V., Carvalho, J., Barreiros, M.A., Coutinho, M.L., Salas-Colera, E., Vigário, R. 2022. Contribution to the Understanding of the Colour Change in Bluish-Grey Limestones. *Heritage 5(3)*, 1479–1503. https://doi.org/10.3390/heritage5030078

Tuğrul, A. 1995. *The Effects of Weathering on The Engineering Properties of Basalts in The Niksar Region*. PhD. thesis, Istanbul University, Istanbul [In Turkish].

Tuğrul, A. 2004. The Effect of Weathering on Pore Geometry and Compressive Strength of Selected Rock Types from Turkey. *Engineering Geology 75(3–4)*, 215–227. https://doi.org/ 10.1016/j.enggeo.2004.05.008

Vogel, D.E. 1975. Precambrian Weathering in Acid Metavolcanic Rocks from the Superior Province, Villebon Township, South-Central Québec. *Canadian Journal of Earth Sciences 12 (12)*, 2080–2085. https://doi.org/10.1139/e75-183

Whitlock, C.H., Brown, D.E., Chandler, W.S., Di Pasquale, R.C., Meloche, N., Leng, G.J., Gupta, S.K. 2000. *Release 3 NASA Surface Meteorology and Solar Energy Data Set for Renewable Energy Industry Use*, Proceedings of Rise and Shine. In: *The 26th Annual Conference of the Solar Energy Society of Canada Inc. and Solar*. Nova Scotia, Canada.

Winkler, E.M. 1966. Important Agents of Weathering for Building and Monumental Stone. *Engineering Geology 1(5)*, 381–400. https://doi.org/10.1016/0013-7952(66)90003-2

Yool, A.I.G., Lees, T.P., Fried, A. 1998. Improvements to the Methylene Blue Dye Test for Harmful Clay in Aggregates for Concrete and Mortar. *Cement and Concrete Research 28(10)*, 1417–1428. https://doi.org/10.1016/S0008-8846(98)00114-8